Vein Related Mass Transport in the Ritter Range Roof Pendant during Late Cretaceous Contact Metamorphism

Cory Hanson

Advised by:
Dr. Penniston-Dorland
Dr. Piccoli
Dr. McDonough

May, 2009

Abstract

A mass balance consideration of quartz-amphibole veins interpreted to have formed during peak metamorphic conditions (~2 kbar and 500 °C) in an andesitic meta-volcanic layer in the Ritter Range Roof Pendant suggests that vein material was derived both from cm-scale diffusion from the surrounding wall rock and from deposition of material from a far-field source. Changes in the mineralogy and mineral chemistry of the altered region surrounding the veins, referred to as selvages, relative to their unaltered wall rock protolith suggest that selvages experienced mass loss. The vein and selvage assemblage experienced a net gain of material relative to the unaltered wall rock. Consideration of the mass balance of individual elements in conjunction with patterns in the concentration of these elements in the wall rock, selvage, and vein allow conclusions to be drawn regarding of the amount of each element derived from far-field sources.

Constraints on mass transfer are crucial to understanding metamorphic fluid conditions and behavior. Investigation of fluid-rock interaction in metavolcanic roof pendants can provide insight into the processes involved in ore generation in similar environments. In addition, a synthesized understanding of mass transfer during metamorphic fluid infiltration and how these processes change with rock type and other environmental conditions can teach us about the sources, paths, and quantities of metamorphic fluids (Ague, 1994; Masters and Ague, 2005).

Table of Contents

Table of Contents: Figures

Introduction

Veins are common features in metamorphic rocks, constituting nearly a third of some amphibolite facies metapelites (Ague, 1994). Veins are fossilized fractures in rock which served as regions of preferential flow for metamorphic fluids (Ague, 1994; Oliver and Bons, 2001). Vein material is derived from the following processes: (1) diffusion of material from the surrounding wall rock driven by pressure and/or concentration gradients created by the proximity of an open fracture and (2) precipitation of material dissolved in metamorphic fluids driven by variations in temperature, pressure, or chemical conditions along the path of the fluid (Oliver and Bons, 2001; Ague, 2003). Veins are potential paths for the transfer, removal, and/or deposition of material mobilized by metamorphic fluids and regions of local re-arrangement of material due to pressure and/or concentration gradients. Distinguishing the quantity of an element derived from the surrounding wall rock from that derived from a far-field source is fundamental to understanding the degree of mobilization that element experiences by interaction with an infiltrating metamorphic fluid. This information can also be used to determine characteristics of the infiltrating fluid including composition and a time integrated fluid flux (Ague, 2003).

In metamorphic systems, fractures are regions of enhanced metamorphic fluid flow. When fracture flow focuses metamorphic fluids into spatially limited channels, pervasive flow along mineral grain boundaries is limited and the original composition of the rock remains relatively unaltered in areas distant from fractures. Selvages are regions of alteration surrounding veins that commonly occur on a mm to m scale. Thus both an unaltered protolith and a region altered by infiltrating metamorphic fluid can be preserved in veined rock. This makes veining a powerful window into element behavior in hydrothermal environments under metamorphic pressure and temperature conditions.

Studies such as Penniston-Dorland and Ferry (2008) suggest mobility of rock forming elements out of the selvage and that certain elements, particularly silicon, are mobilized on a regional scale by infiltrating fluid and deposited in the vein. Other elements have been suggested to be regionally mobilized by infiltrating fluids such as some alkali and metallic elements (Ague, 1994; Ague 2003; Masters and Ague, 2005). Studies have tended to focus on quartz-dominated veins in metapelitic rocks in low to mid grade metamorphic conditions.

This study looks at element mobility in mineralogically diverse veins in metavolcanic that formed under greenschist metamorphic conditions. Patterns in the concentration ratios of a suite of elements are considered in conjunction with mineral compositions and suggested element mobility in other metamorphic environments to constrain the volume loss experienced by the selvage. This is used in a mass balance equation which quantifies the amount of individual element mass loss or gain during vein fill regardless of volume and density changes associated with metasomatism (Gresens, 1966, Grant 1986, Ague 1994, Penniston-Dorland 2008). The results of the mass balance equation are considered in conjunction with literature on metasomatism in other metamorphic environments and patterns in each element's concentration ratios to make conclusions regarding the source of elements in the vein.

Geologic Background

The veins considered in this study are found in a metavolcanic layer in the lower section of the Ritter Range Roof Pendant in the Ansel Adams Wilderness Area north-east

of Mammoth Lakes, CA. This is a 20 by 30 km roof pendant making it one of the largest roof pendants in the Sierra Nevada batholith (Hanson et al., 1993). Normal faults place the younger upper section adjacent to the older lower section. The upper section consists of terrestrially deposited ash tuffs and collapse breccia which fill a large caldera near the center of the pendant (Hanson et al., 1993). The lower section consists of mostly near shore and off shore metavolcanics and around 40 calc-silicate layers (Hanson et. al, 1993). The lower section layering strikes NW/SE and dips steeply to the SW.

The Kuna Crest Granodiorite (91Ma) is the principle intruding body into the Ritter Range Roof Pendant (Hanson et al., 1993; Sorensen et al., 1998). Other intrusive bodies are present in the pendant and have been dated at 100Ma (Hanson et al., 1993). The normal faulting places the upper and lower sections of the pendant adjacent to one another and is cut by the Kuna Crest. Normal faulting must have occurred between the age of the upper section (determined to be 100 Ma based on Rb-Sr and U-Pb) and the emplacement of the Kuna Crest at 91Ma. Intrusion of the Kuna Crest Granodiorite is believed to have caused the peak degree of metamorphism experienced by the pendant at 2 kilobars and 450-500°C (Hanson et al., 1993).

The outcrop that is the focus of this study is located in the lower section near the foot of Garnet Lake beneath Mount Ritter. A map of the field locality can be seen in Figure 1. This locality is approximately half of a kilometer from the nearest exposed outcrop of the Kuna Crest Granodiorite. Subsurface proximity of the Kuna Crest is not known. The amphibole/quartz veins this study focuses on are interpreted to have formed during peak metamorphic conditions based on vein mineral assemblages and characteristics described by Hanson et al. (1993). The layer also contains small (~1mm thick) quartz veins and small amphibole veins as well as epidote blebs, pods, and streaks. Smaller veins tend to not have selvages.

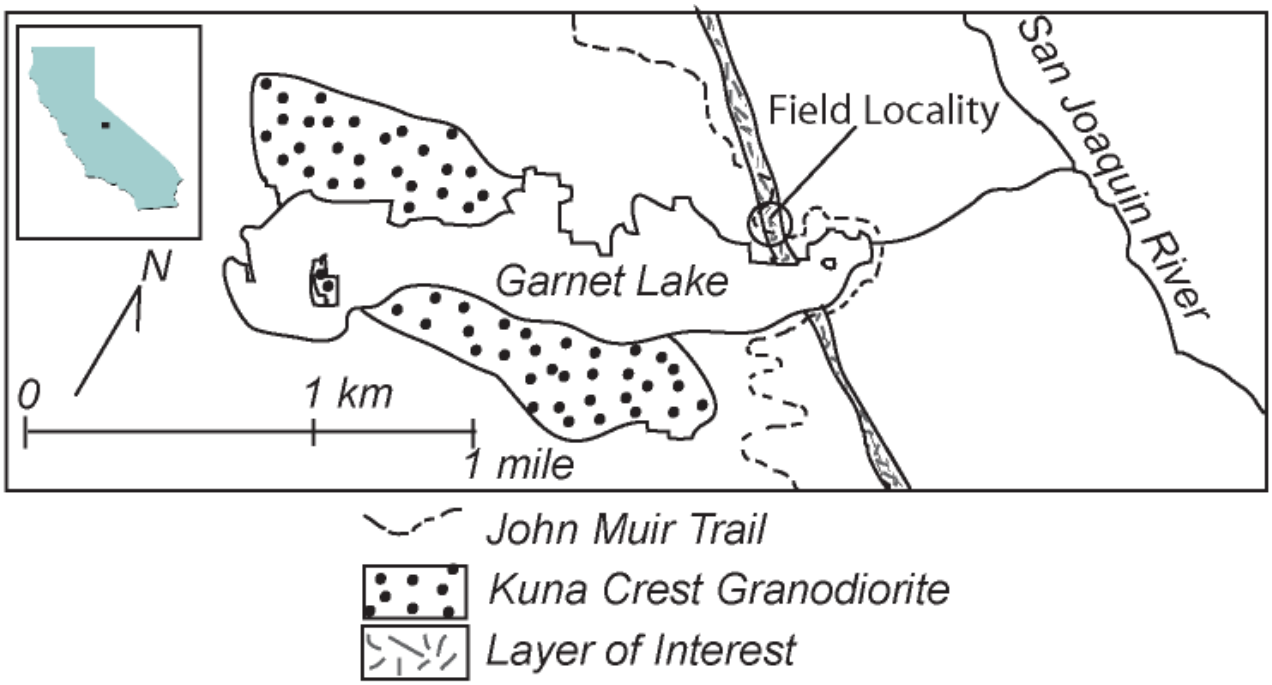

Figure 1. *Field Locality Map. Lower section of the Ritter Range Roof Pendent. Based on Hanson et al. (1993).*

Methods

Outcrop Measurements

A 24 meter traverse of outcrop was measured using a tape measure laid across the outcrop perpendicular to the average vein orientation. Distances and thicknesses of all veins and other features that fell under the tape were recorded. Uncertainties for these measurements are assumed to be 3 millimeters because the smallest increment on the tape measure used is 1/8" (~3mm). The outcrop exposure on which measurements were made is approximately perpendicular to the dip of the layer. Distance measurements can be exaggerated if the plane of the vein and the outcrop surface are not perpendicular. The greater the deviation from perpendicular is the greater the exaggeration in the measured distance. This means that calculated thicknesses and measured lengths are, at worst, maximum constraints. Assuming each region experienced similar degrees of exaggeration no bias is imparted to the ratios of these regions. Therefore, the calculated percentages of vein and selvage exposed across the measured length should be accurate. A summary of field measurement data can be found in Appendix A.

Thickness Measurements

Hand samples containing a single vein, its associated selvage, and the surrounding wall rock were collected from the exposure. An image of the primary hand sample used in this study can be found in Figure 2. Vein and selvage thicknesses in this hand sample were measured at a greater level of detail. These measurements were made by beginning at one "corner" of the sample and measuring vein and selvage thickness every centimeter along the vein. A millimeter-scale ruler was used to make the measurements. Due to the exaggeration that may exist from variations from this perpendicular geometry, these measurements are maximum constraints. However, the veins are very nearly perpendicular to all exposures on the hand samples so these measurements are considered a reasonable measure of thicknesses for the purposes of this study. A summary of hand sample measurements can be found in Figure 3.

	Vein	Selvage	Vein/Selvage
Average	1.0	0.6	1.7
1 σ	0.3	0.2	0.6

Figure 3. *Vein thickness measurements made on hand sample RQ0853*

Figure 2. *A photo of hand sample RQ0853*

Phase Abundance and Chemistry Determination

Hand samples were cut and sent to Texas Petrographics, Inc. for thin section creation. Three sets of polished 30 micron and 100 micron sections were made. Two of these sets contained selvage and vein material. The third set contained wall rock material. The wall rock section was made from a hand sample showing no signs of alteration and taken as distant as possible from any visible veining or other region of alteration.

Mineral assemblages and petrographic observations were made on thin sections using petrographic microscopy and backscatter electron imaging (BSE) on an electron probe microanalyzer (EPMA). Mineral abundances were quantified through point counting performed with BSE imaging and energy dispersive spectrometry (EDS). Uncertainties for mineral abundances were determined by the method described by Van der Plas and Tobi (1965). Phase abundances can be found in Figure 4.

The major element chemistry of major mineral phases was measured using wavelength dispersive spectrometry (WDS). Standard counting statistics were used to calculate uncertainties for these measurements. Several phases with little to no variation in crystal chemistry were not analyzed. These phases are quartz, calcite, apatite, titanite, zircon, chalcopyrite, and wall rock ilmenite. These phases are assumed to have stoichiometric composition. This assumption is expected to have an error associated with it equal to or less than the error generated by combined heterogeneity and analytical uncertainty. Additionally, with the exception of quartz, these phases are trace phases and as such do not contribute greatly to the overall element budget of the rock. A summary of major constituent phase chemistry can be found in Figure 6.

Laser ablation inductively coupled plasma mass spectrometry (LA-ICP-MS) was used to determine trace element chemistry of major phases in terms of modal abundance and trace phases that likely control the budgets of some trace elements. Uncertainties for LA-ICP-MS results are assumed to be ten percent. Several phases were not analyzed for trace element composition due to analytical limitations. These phases are quartz, zircon, apatite, chalcopyrite, selvage calcite, wall rock ilmenite, and wall rock biotite. In this study, these phases are assumed to not contribute significantly to the budget of the suite of trace elements measured in this study. With the exception of quartz, these phases were not analyzed because they occur as grains with diameters of less than five microns; these grains are too small to be analyzed on the LA-ICP-MS. Quartz does not couple well with the laser in LA-ICP-MS. A summary of measured trace element composition for analyzed phases can be found in Figure 7.

With the exception of quartz and wall rock biotite, these phases are trace phases and as such they are minor contributors to the element budget of the three regions studied. Quartz is not expected to have an appreciably large concentration of any trace elements analyzed in this study. Metamorphic biotite is suggested to have negligible (<1 ppm) concentrations of rare earth elements (REEs), Y, Th, and U (Pyle et al., 2001). Cesium, however, is expected to be relatively abundant in biotite as a substitute for potassium. Additionally, trace minerals not analyzed in this study may contain high enough concentrations of some trace elements as to appreciably affect the budget of those elements in the rock. For instance, apatite often contains relatively large (~1000 ppm) concentrations of light rare earth elements (LREEs) (Pyle et al, 2001). Finally, trace element budgets that rely heavily on a trace phase (such is likely in the case of apatite

with LREEs or zircon with zirconium, uranium, thorium, and lead) are vulnerable to the "nugget effect." This suggests that relatively small under or overestimations of trace phase abundances can significantly alter the concentrations of trace elements whose budgets are strongly dictated by that phase.

Bulk Rock Analysis

Two samples of selvage and three samples of wall rock material were collected from hand samples using a rock saw and Dremel sanding tool. These were sent to SGS Mineral Services for bulk-rock x-ray fluorescence (XRF) for major constituent element determination and for the analysis by bulk-rock inductively coupled plasma mass spectrometry (ICP-MS) for trace element concentration determination. The averages of results are used for the composition of selvage and wall rock in this study with the exception of Ta because it was beneath the lower limit of detection via ICP-MS. Heterogeneity and variability of wall rock and selvage concentrations were calculated as the standard deviation of these measurements from their mean. Vein material is difficult to separate without biasing the sample due to heterogeneity in vein composition perpendicular to the plane of veining. As a result, in-situ phase measurements and phase abundance values are used to calculate the bulk rock composition of the vein. Both measured and calculated bulk rock compositions for each region can be found in Figure 8.

Density Determination

Rock density was determined through two methods. In the first, density calculations were made by taking the average of mineral densities (Holland and Powell, 1998) weighted by mineral abundance. Mineral densities were estimated using either average values or values that reflect the major element composition of the phase. Uncertainties for these densities were calculated by propagation of point counting uncertainty. Additional uncertainties caused by the assumption of an average mineral density are unquantifiable. Wall rock and selvage densities were also calculated by measuring the mass and volume of several samples of each region. These measurements were performed using a scale and a 1mL incremented graduated cylinder. The average density calculated with these measurements is used in this study for these regions. This second method has fewer uncertainties and the values for wall rock and selvage density obtained using this method are used in the subsequent calculations in this paper. However, vein material is brittle and difficult to separate so the first method of density determination is relied on for calculations involving vein density in this study. These densities can be found in Figure 5.

Mass Balance

The mass balance analysis of this wall rock, selvage, and vein assemblage is made for individual elements. Thus this analysis can determine the proportion of a given element derived from non local sources. The following equation can be used to calculate how much mass of an element per volume of vein was brought into or taken from (depending on the sign of the value) the vein/selvage system:

1)

$$\Delta C_i * x^{sel} * \rho^{sel} + C_i^{vein} * x^{vein} * \rho^{sel} = C_i^{ext}$$

where x^{sel} is the total thickness of the selvage on both sides of the vein, x^{vein} is the thickness of the vein, C_i^{vein} is the concentration of element *i* in the vein in mass of element per area of vein/selvage complex, C_i^{ext} is the concentration of externally derived mass of element *i* in mass of element per unit mass of vein/selvage assemblage, and ΔC_i is the

change in concentration of that element in the selvage relative to the wall rock in mass of element per unit mass of selvage. ΔC_i is properly defined as:

2)

$$\Delta C_i = \left[\left(\frac{C^{wr}}{C^{sel}} \right)_{ref} \left(\frac{C^{sel}}{C^{wr}} \right)_i - 1 \right] C_i^{wr}$$

where C^{wr} is concentration of an element in the wall rock and C^{sel} is the concentration in the selvage and *ref* denotes an element that was immobile during alteration, fracture, vein fill, and fluid infiltration. The term $(C^{wr}/C^{sel})_{ref}$ uses a reference element believed to be immobile during fluid infiltration and vein fill to estimate the degree of volume change the selvage experienced during formation (Gresens, 1966; Grant, 1986; Ague, 1994). Net volume change in the selvage relative to the wall rock is extremely likely because the selvage is a region of metasomatic alteration of the protolith wall rock. Unaccounted for, this type of volume change skews the fractional change in concentration of elements between the selvage and wall rock. The volume change can be calculated using the following equation (Penniston-Dorland and Ferry, 2008):

3)

$$\Delta V = \frac{\rho^{wr}}{\rho^{sel}} * \left(\frac{C^{wr}}{C^{sel}} \right)_{ref} - 1$$

where ΔV is the fractional change in volume of the selvage .

Gresens (1966) used a composition-volume diagram to support assumptions made about the immobility of elements. Papers published by Baumgartner and Olsen (1995) and Ague and Van Haren (1996) discuss more refined but essentially similar methods to estimate immobile elements:

1) Eliminate major constituent elements of minerals within the vein
2) Eliminate elements shown to be mobile in environments similar to that of the study
3) Eliminate elements with relatively large uncertainties
4) Choose a suite of elements from those remaining with overlapping or very similar C_i^{wr}/C_i^{sel} ratios

Grant (1986) also suggests that it is desirable to consider elements that are geochemically dissimilar to ensure that the overlapping $C_{i,sel}/C_{i,wr}$ ratios (or concentration ratios) are not a result of the similar degrees of mobility of each element.

Measurements and Observations

Layer and Vein Description

The rock unit containing the veins of interest in this study is an andesitic metavolcanic layer. These volcanics are interpreted to have been deposited subaqueously during the Jurassic-Triassic (Hanson et al., 1993). The layer strikes northwest/southeast and dips steeply to the southwest. The layer is composed primarily of plagioclase with smaller amounts of amphibole and biotite and trace amounts of ilmenite, apatite, quartz, zircon, titanite and chalcopyrite. Plagioclase occurs as millimeter-scale phenocrysts and as a large portion of the matrix. Amphibole and biotite are only found in the matrix. Mineral abundances were determined using point counting and results are listed in Figure 4. The density of this rock is 2.8 ± 0.1 g/cm^3 (Figure 5).

Veins in this layer are sub-planar and nearly parallel. They tend to be orientated northeast/southwest (nearly perpendicular to

	Selvage		Wall Rock		Vein	
Selvage	**Volume %**	**2σ**	**Volume %**	**2σ**	**Volume %**	**2σ**
Amphibole	17	4	17	3	52	5
Plagioclase	75	4	68	5	10	3
Biotite	0	-	11	3	0	-
Quartz	0.5	0.7	4	2	28	4
Ilmenite	0.6	0.8	0.8	0.9	0.6	0.8
Apatite	0.5	0.7	0.2	0.5	0	-
Calcite	0.7	0.8	0	-	2	2
Titanite	2	1	0	-	0.6	0.8
Epidote	4	2	0	-	3	2
Pyroxene	0	-	0	-	2	1
Chalcopyrite	0	-	0.1	0.4	0	-
Chlorite	0	-	0	-	1	1

Figure 4. *Mineral abundances by region.*

layer strike) and crosscut foliation. The veins vary in thickness from less than a millimeter to around 5 centimeters. Only the thicker veins have visible selvages. The veins are relatively short in extent (less than 5 meters) and are not observed to cross layer boundaries in outcrop. Spacing between veins can range from a few centimeters to tens of centimeters. Veins with selvages tend to be separated by at least a meter. Thicker veins with selvages, which this study focuses on, are dominated by amphibole and quartz. Plagioclase, epidote, calcite, pyroxene, and chlorite are minor phases. Titanite and ilmenite are trace phases. Mineral abundances in the vein were determined using point counting and are listed in Figure 4. The density of the veins is 3.0 ± 0.2 g/cm^3 (Figure 5).

Selvages are visually distinguishable as bleached regions on either side of a vein. They retain the porphyritic texture of the wall rock; however, they are lighter in color. They vary in thickness from 0 to 11mm (see Appendix A). Variation of selvage thickness along the vein is frequent and can be sudden or gradual. No pattern was discerned from selvage thickness variation. Selvages comprise plagioclase, amphibole, epidote, titanite, ilmenite, and zircon. Plagioclase dominates the selvage assemblage and occurs as both mm-scale phenocrysts and in the matrix. Other phases are present only in matrix. Mineral abundances in the selvage were determined using point counting and are listed in Figure 4. The density of the selvage is 2.4 ± 0.2 g/cm^3 (Figure 5).

	calculated		measured	
	density (g/cm3)	**2σ (g/cm3)**	**density (g/cm3)**	**2σ (g/cm3)**
Vein	3.0	0.24	-----	-----
Selvage	2.8	0.19	2.4	0.2
Wall Rock	2.8	0.12	2.81	0.02

Figure 5. *Densities by region. "Calculated" values obtained using mineral assemblage and average mineral densities. "Measured" values obtained by mass and volume measurements of multiple samples.*

Wall Rock

	SiO_2	Al_2O_3	TiO_2	FeO	CaO	Na_2O	K_2O	MnO	MgO
Amphibole	45.0	10.01	0.44	21.0	11.27	1.07	0.33	0.418	7.84
+/-	0.1	0.06	0.01	0.1	0.05	0.03	0.01	0.000	0.08
Chalcopyrite	0	0	0	47	0	0	0	0	0
+/-	0	0	0	0	0	0	0	0	0
Quartz	100	0	0	0	0	0	0	0	0
+/-	0	0	0	0	0	0	0	0	0
Biotite	35.7	15.85	1.90	23.2	0.182	0.07	8.79	0.22	8.29
+/-	0.1	0.07	0.02	0.1	0.002	0.01	0.05	0.03	0.08
Ilmenite	0	0	53	47	0	0	0	0	0
+/-	0	0	0	0	0	0	0	0	0
Apatite	0	0	0	0	55	0	0	0	0
+/-	0	0	0	0	0	0	0	0	0
Plagioclase	61.0	24.65	-	0.18	6.15	7.94	0.18	-	-
+/-	0.1	0.09	-	0.02	0.04	0.05	0.01	-	-

Selvage

	SiO_2	Al_2O_3	TiO_2	FeO	CaO	Na_2O	K_2O	MnO	MgO
Amphibole	46.7	8.77	0.35	20.6	11.76	0.90	0.34	0.514	8.20
+/-	0.1	0.05	0.01	0.1	0.05	0.02	0.01	0.001	0.08
Epidote	37.9	25.46	-	11.41	23.39	-	-	0.24	0.03
+/-	0.1	0.08	-	0.09	0.07	-	-	0.05	0.07
Calcite	0	0	0	0	56.03	0	0	0	0
+/-	0	0	0	0	0	0	0	0	0
Quartz	100	0	0	0	0	0	0	0	0
+/-	0	0	0	0	0	0	0	0	0
Titanite	30	5	30	2	27	0	0	0	0
+/-	0	0	0	0	0	0	0	0	0
Ilmenite	0.12	0.01	49.91	44.6	0.10	-	-	4.37	0.11
+/-	0.01	0.01	0.05	0.2	0.01	-	-	0.08	0.01
Apatite	0	0	0	0	55	0	0	0	0
+/-	0	0	0	0	0	0	0	0	0
Plagioclase	56.7	27.48	-	0.10	9.59	6.32	0.07	-	-
+/-	0.1	0.10	-	0.01	0.06	0.04	0.01	-	-

Vein

	SiO_2	Al_2O_3	TiO_2	FeO	CaO	Na_2O	K_2O	MnO	MgO
Amphibole	44.3	11.41	0.072	18.4	12.07	1.20	0.54	0.4233	9.25
+/-	0.1	0.07	0.002	0.1	0.05	0.03	0.02	0.0004	0.09
Epidote	37.8	25.27	-	11.78	23.38	-	-	0.24	0.017
+/-	0.1	0.08	-	0.09	0.07	-	-	0.05	0.005
Chlorite	28.59	19.48	-	23.3	0.096	-	-	0.58	16.5
+/-	0.09	0.08	-	0.1	0.008	-	-	0.04	0.1
Pyroxene	51.3	0.29	0	16.5	23.76	0.16	0.012	1.06	7.36
+/-	0.1	0.01	0	0.1	0.06	0.02	0.006	0.05	0.07
Calcite	0	0	0	0	56	0	0	0	0
+/-	0	0	0	0	0	0	0	0	0
Quartz	100	0	0	0	0	0	0	0	0
+/-	0	0	0	0	0	0	0	0	0
Titanite	30	5	30	2	27	0	0	0	0
+/-	0	0	0	0	0	0	0	0	0
Ilmenite	0.01	0.005	49.58	44.0	0.011	0	0	5.90	0.08
+/-	0.01	0.005	0.05	0.2	0.008	0	0	0.08	0.01
Plagioclase	54.6	29.2	-	0.27	11.05	5.11	0.31	-	-
+/-	0.1	0.1	-	0.02	0.07	0.03	0.02	-	-

Figure 6. *Mineral chemistry by region measured by WDS-EPMA. Values are given as oxide weight percent. Italicized phases are unmeasured phases assumed stoichiometric for the purposes of this study. '-' denotes an element that was not measured for that phase and assumed 0.*

Wall Rock

	Ti	Mn	Sc	V	Sr	Y	Zr	Nb	Cs	Ba	La	Ce	Pr	Nd	Sm
Amphibole	5752	3938	53	674	16	22	4	2	1	103	0.1	0.6	0.2	1	0.8
Plagioclase	130	-	-	20	616	0.3	3	0.1	1	255	0.3	0	0.0	0.2	0.1

	Eu	Gd	Tb	Dy	Ho	Er	Tm	Yb	Lu	Hf	Ta	Pb	Th	U
Amphibole	0.5	2	0.4	3	0.8	2	0.3	3	0.3	0.2	0.08	3	0.005	0.03
Plagioclase	0.1	0.03	0.01	0.08	0.015	0.04	0.01	0.02	0.03	0.08	-	16	0.01	0.03

Selvage

	Ti	Mn	Sc	V	Sr	Y	Zr	Nb	Cs	Ba	La	Ce	Pr	Nd	Sm
Amphibole	2490	4158	31	434	132	46	187	2	-	46	0.7	2	0.6	3	1
Epidote	407	2030	70	205	1047	208	173	0.2	-	62	593	1193	144	642	129
Titanite	--	3760	16	812	28	66	69	278	-	160	4	23	5	33	12
Ilmenite	299210	33474	-	352	-	12	3	123	-	-	-	0.07	0.04	1	0
Plagioclase	61	303	-	16	891	0.5	8	0.03	1	156	0.3	0.7	0.1	0.3	0.2

	Eu	Gd	Tb	Dy	Ho	Er	Tm	Yb	Lu	Hf	Ta	Pb	Th	U
Amphibole	0.7	2	0.7	6	2	6	0.9	7	1.0	6	0.2	5	0.4	1
Epidote	37	99	12	54	8	15	2	9	1	5	-	41	98	12
Titanite	20	13	2	12	3	6	0.9	7	1	3	8	4	0.5	4
Ilmenite	-	-	0.5	0.7	0	0.4	-	0.2	0	0	5	12	0.05	0.4
Plagioclase	0.09	0.04	0.01	0.07	0.02	0.01	0.004	0.2	0.02	0.2	0	18	0.07	0.04

Vein

	Ti	Mn	Sc	V	Sr	Y	Zr	Nb	Cs	Ba	La	Ce	Pr	Nd	Sm
Amphibole	1198	4897	16	391	12	10	2	0.5	0.0	43	0.02	0.2	0.07	0.4	0.4
Epidote	1977	1979	29	696	773	109	34	0.06	-	0	5	12	2	11	6
Titanite	366	5850	16	350	12	4	0.3	-	-	75	0.0	0.2	0.03	0.2	0.2
Ilmenite	297232	46429	-	214	-	-	-	225	12	-	-	0	0.06	0	-
Pyroxene	135	9006	18	98	10	0.1	0.6	-	-	1	0.03	0.8	0.00	0.008	0.03
Calcite	83	6509	2	40	201	6	0.2	0.04	0.06	9	0.0	0.02	0.00	0.008	0.009
Plagioclase	-	-	-	-	919	0.02	-	0.02	3	324	-	0.0	0.0	0.0	0.02
Chlorite	114	7617	2	410	4	0.03	-	-	0.8	102	0.01	-	0.0	0.0	0.2

	Eu	Gd	Tb	Dy	Ho	Er	Tm	Yb	Lu	Hf	Ta	Pb	Th	U
Amphibole	0.3	0.7	0.1	1	0.3	1	0.2	2	0.4	0.03	0.02	2	0.001	0.008
Epidote	8	9	2	15	3	12	2	17	3	1	0.002	30	0.02	2
Titanite	0.5	0.3	0.07	0.5	0.1	0.6	0.05	0.3	0.1	0.006	0.005	2	0.0008	0.009
Ilmenite	-	1	0.0	0.0	0.0	0.0	0.02	0.0	0.0	0.4	4	-	0.0	174
Pyroxene	0.010	0.01	0.002	0.02	0.006	0.02	0.009	0.1	0.07	0.03	0.02	2	0.0002	0.002
Calcite	0.03	0.06	0.02	0.3	0.2	1	0.3	4	1.0	0.01	0.002	7	-	0.004
Plagioclase	0.10	0.07	0.0	0.003	0.0	0.01	0.002	0.0	0.004	0	0	17	0.0	0.001
Chlorite	0.01	0.01	0.006	0.01	0.002	0.0	0.008	0.003	0.004	0.01	0.006	10	0.0	0.009

Figure 7. *Mineral trace element compositions by region measured by LA-ICP-MS. All measurements reported in parts per million (ppm) by weight. '-' denotes that the measurement was beneath the lower limit of detection and assumed to be 0 for this study. Uncertainties assumed to be 10%.*

Mineralogy and Mineral Chemistry

The average major element composition of each mineral in each region can be found in Figure 6. The average trace element composition of each phase in each region is shown in Figure 7. Comparing the composition and trace element concentrations of phases that appear in multiple regions is a useful way to glean information about the budget, partitioning, and behavior of various elements. For these considerations the most useful phases in this study are plagioclase, amphibole, epidote, titanite, and ilmenite.

Plagioclase is present in all three regions of the rock and contributes significantly to the bulk rock composition of both Na and Ca in this study. Plagioclase dominates the Na budget of all three regions; however, Ca has very significant additional contributions from amphibole, calcite, titanite, pyroxene, and epidote when present. Wall rock plagioclase has 37-85 % albite component. Selvage plagioclase is 34-67 % albite component. Vein plagioclase is 28-37 % albite component. A ternary plot of plagioclase compositions can be found in Appendix B. In addition to element abundance at the time of crystal growth, temperature and pressure conditions are known to influence the albite composition of plagioclase. Disregarding this complication, The decreased Na content of plagioclase in the selvage suggests that either Na was preferentially removed from the selvage or that Ca was preferentially added to the selvage or some combination of the two. The even lower Na content in vein plagioclase supports the former.

Plagioclase also represents a significant portion of the Sr budget and Pb budget, especially in the wall rock. Sr concentrations in plagioclase increase significantly from wall rock (616 ppm) to selvage (819 ppm) to vein (919 ppm). Additionally, the selvage and vein contain other phases with significant Sr content. These observations suggest that Sr may have experienced a net influx of material from a far-field source. Lead does not significantly change concentration in plagioclase. However, a sharp increase in the concentration of lead in the vein is observed. This is attributed to the high Pb content of vein chlorite.

Amphibole (calcic ferro-edenite) influences the budget for many elements in these rocks, however, it does not dominate the budget of any of them. Changes observed in the composition and trace element concentrations of amphibole do not appear to follow any systematic behavior.

Epidote is present in the selvage and vein but not the wall rock. The budget for LREEs is dominated by epidote in these regions. Vein epidote has significantly lower LREE content than selvage epidote. The low concentrations of LREEs in vein epidote suggest that LREEs were not mobile during vein formation.

Epidote is also useful for looking at thorium and cerium. Selvage epidote contains an average of ~98 ppm Th and ~1193ppm Ce, while vein epidote contains only ~.02 ppm Th and ~12ppm Ce. Of note is that epidote is not present in the wall rock and it is likely that epidote formed during alteration of the selvage and vein fill. In addition, thorium has a very high C_i^{wr}/C_i^{vein} ratio (shown in Figure 9). These observations suggest very little thorium or cerium was locally transported into the vein.

Biotite is the dominant potassium bearing phase in the wall rock. It is not present in the selvage or vein or no other major potassium bearing phase replaces it. This suggests that potassium was removed by an infiltrating metamorphic fluid.

Bulk Rock Chemistry

The calculated and measured bulk rock chemical composition of each region is

	Wall Rock				Selvage				Vein		
	In Situ		Bulk Rock		In Situ		Bulk Rock		In Situ		
		2σ		2σ		2σ		2σ		2σ	
Ca	0.045	0.002	0.0467	0.0006	0.10	0.01	0.070	0.006	0.06	0.01	**g / g**
Na	0.020	0.001	0.0181	0.0002	0.021	0.001	0.018	0.002	0.005	0.001	**g / g**
Al	0.052	0.003	0.050	0.001	0.071	0.004	0.055	0.005	0.028	0.003	**g / g**
Si	0.260	0.012	0.258	0.003	0.29	0.02	0.26	0.02	0.24	0.02	**g / g**
K	0.0047	0.0002	0.0058	0.0001	0.0006	0.0001	0.0008	0.0001	0.0011	0.0001	**g / g**
Ti	0.0055	0.0002	0.0061	0.0001	0.01	0.01	0.0054	0.0005	0.004	0.004	**g / g**
Fe	0.058	0.002	0.059	0.001	0.05	0.01	0.031	0.003	0.07	0.01	**g / g**
Mg	0.014	0.001	0.0156	0.0002	0.011	0.002	0.027	0.002	0.029	0.003	**g / g**
Mn	0.00080	0.00003	0.00106	0.00001	0.001	0.001	0.010	0.001	0.002	0.001	**g / g**
Sc	10	1	23.3	0.2	11	3	18.0	0.2	323	210	**µg / g**
V	144	14	254	3	144	29	155	2	64040	42874	**µg / g**
Sr	625	74	650	7	848	93	851	9	767	423	**µg / g**
Y	4.4	0.5	23.1	0.2	25	7	18.5	0.2	13	4	**µg / g**
Zr	2.1	0.2	103	1	60	11	111	1	2	1	**µg / g**
Nb	0.45	0.04	4.00	0.04	8	5	4.00	0.04	2	3	**µg / g**
Cs	0.00	0.00	4.00	0.04	1.2	0.1	0.400	0.004	121	81	**µg / g**
Ba	242	26	576	6	149	16	159	2	15912	10653	**µg / g**
La	0.43	0.05	15.3	0.2	37	17	16.2	0.2	1	1	**µg / g**
Ce	0.79	0.08	30.9	0.3	74	35	33.1	0.3	0.5	0.2	**µg / g**
Pr	0.10	0.01	4.08	0.04	9	4	4.29	0.04	0.10	0.04	**µg / g**
Nd	0.64	0.05	17.5	0.2	41	19	18.1	0.2	0.6	0.2	**µg / g**
Sm	0.24	0.02	4.10	0.04	9	4	4.15	0.04	26	17	**µg / g**
Eu	0.26	0.02	1.27	0.01	3	1	1.29	0.01	2	1	**µg / g**
Gd	0.33	0.03	4.85	0.05	7	3	4.30	0.04	3	2	**µg / g**
Tb	0.08	0.01	0.75	0.01	0.9	0.4	0.650	0.007	1	1	**µg / g**
Dy	0.65	0.07	4.39	0.04	5	2	3.59	0.04	3	2	**µg / g**
Ho	0.15	0.02	0.88	0.01	0.9	0.3	0.735	0.007	0.6	0.2	**µg / g**
Er	0.44	0.05	2.56	0.03	2	1	2.05	0.02	1.0	0.2	**µg / g**
Tm	0.08	0.01	0.373	0.004	0.3	0.1	0.310	0.003	1	1	**µg / g**
Yb	0.56	0.06	2.50	0.03	2.3	0.5	2.00	0.02	2.4	0.5	**µg / g**
Lu	0.08	0.01	0.357	0.004	0.3	0.1	0.305	0.003	1.0	0.4	**µg / g**
Hf	0.08	0.01	3.00	0.03	1.9	0.4	3.00	0.03	2	2	**µg / g**
Ta	0.014	0.002	-	-	0.3	0.2	-	-	1	1	**µg / g**
Pb	18	2	14.0	0.1	19	2	16.0	0.2	1506	1009	**µg / g**
Th	0.030	0.003	2.30	0.02	6	3	2.70	0.03	0.0014	0.0004	**µg / g**
U	0.028	0.003	0.920	0.009	1.1	0.4	0.875	0.009	3	2	**µg / g**

Figure 8. *Bulk rock chemical composition measured by XRF (Ca-Mn) and LA-ICP-MS (Sc-U).*

summarized in Figure 8. The measured bulk rock chemical composition of each region is used in further analysis. The calculated bulk rock composition for the vein is always used due to the lack of directly measured values.

The bulk rock chemistry of the unaltered volcanic material in this layer is similar to volcanic layers measured by Hanson et al. (1993). A summary of the oxide weight percent of this rock is in Appendix C. The most notable difference between the layer in this study and layers discussed by Hanson et al. (1993) is the CaO content of this layer is relatively high. CaO is also found to be exceptionally variable in both Hanson et al. (1993) and this study (31% standard deviation). Hanson et al. (1993) speculates that the variability of CaO in his samples may be due to vein related alteration.

Heterogeneity in the wall rock is an important source of uncertainty. Most elements were found to have heterogeneities resulting in less than a 5% standard deviation of average concentrations (based on multiple bulk rock analyses). Important exceptions to this include: Ca (10%), K (31%), Fe (10%), Mg (14%), Ba (18%), Cs (39%), and Pb (19%). One wall rock sample is drastically controlling the uncertainty of these elements (except for lead). These elements would likely vary drastically in a region of wall rock containing epidotization as is seen in the layer. No such reason to exclude this sample from analysis was found before it was pulverized, however, these large uncertainties (with the exception of lead) would be reduced if this sample were not considered.

The most useful way to compare bulk rock composition in the vein, selvage, and wall rock is to consider the concentration ratios of the three regions. These ratios can be found in Figures 9 and 10. Elements with higher C_i^{wr}/C_i^{vein} ratios were likely less mobilized during vein fill and alteration than those with higher values. An element with a C_i^{wr}/C_i^{sel} ratio less than one is suggested to have been either added to the selvage and/or increased in concentration in the selvage because of the loss of other material from the selvage. Additionally, it is unlikely that these elements were removed from the system by a metamorphic fluid because this would leave the selvage depleted in this element whereas a C_i^{wr}/C_i^{sel} greater than one indicates enhancement. Additionally, elements with C_i^{wr}/C_i^{sel} ratios that are less than one and that have high C_i^{sel}/C_i^{vein} ratios likely experienced less diffusion from the selvage during alteration than similar elements with a lower C_i^{sel}/C_i^{vein}. Careful consideration of all three of these ratios can yield information that allows for grouping of elements based on their mobility.

A chart of the concentration ratios for the elements considered in this study can be found in Figure 10. Similarities in the concentration ratios of the elements Na, Al, Th, Zr, La, Ce, Pr, and Nd suggest that they were mobilized similarly during vein fill and selvage alteration. These elements share a C_i^{wr}/C_i^{sel} that is below one, and very high C_i^{wr}/C_i^{vein} and C_i^{sel}/C_i^{vein} ratios. These ratios suggest that this suite of elements experienced little overall mobility, relatively small degrees of diffusion from the selvage to the vein, and either addition to the selvage by deposition from a metamorphic fluid or increased in composition in the selvage as a result of the loss of other material from the selvage.

Immobile Reference Frame Selection

An suite of potential immobile reference frame elements was selected based on the criteria described in the 'Mass Balance' section of this paper. These elements are suspected to have experienced less diffusion into the vein relative to other elements based on studies in similar environments (Ague, 1994; Masters and Ague, 2005; Penniston-Dorland and Ferry,

	C_i^{wr}/C_i^{sel}		C_i^{wr}/C_i^{vein}		C_i^{sel}/C_i^{vein}	
		2σ		2σ		2σ
Ca	0.67	0.06	0.62	0.07	0.9	0.1
Na	0.99	0.08	4.5	0.6	4.6	0.7
Al	0.90	0.08	2.0	0.2	2.2	0.3
Si	0.98	0.08	0.92	0.08	0.9	0.1
K	7.0	0.6	6.2	0.6	0.9	0.1
Ti	1.1	0.1	1.2	0.9	1.1	0.8
Fe	1.9	0.2	0.58	0.06	0.3	0.0
Mg	0.58	0.05	0.52	0.05	0.9	0.1
Mn	0.11	0.01	0.36	0.07	3.2	0.7
Sc	1.30	0.02	0.07	0.05	0.06	0.04
V	1.64	0.02	0.004	0.003	0.002	0.002
Sr	0.76	0.01	0.8	0.5	1.1	0.6
Y	1.25	0.02	1.7	0.5	1.4	0.4
Zr	0.92	0.01	46	13	49	14
Nb	1.00	0.01	2	2	2	2
Cs	10.0	0.1	0.03	0.02	0.003	0.002
Ba	3.62	0.05	0.04	0.02	0.01	0.01
La	0.95	0.01	15	8	16	9
Ce	0.93	0.01	58	25	63	27
Pr	0.95	0.01	42	15	44	16
Nd	0.97	0.01	31	12	32	12
Sm	0.99	0.01	0.2	0.1	0.2	0.1
Eu	0.98	0.01	0.5	0.3	0.6	0.3
Gd	1.13	0.02	1.6	0.9	1.4	0.8
Tb	1.15	0.02	0.7	0.4	0.6	0.3
Dy	1.23	0.02	1.3	0.6	1.1	0.5
Ho	1.20	0.02	1.5	0.5	1.2	0.4
Er	1.25	0.02	2.5	0.6	2.0	0.5
Tm	1.20	0.02	0.3	0.1	0.2	0.1
Yb	1.25	0.02	1.1	0.2	0.8	0.2
Lu	1.17	0.02	0.4	0.2	0.3	0.1
Hf	1.00	0.01	1.3	0.8	1.3	0.8
Ta	0.05	0.03	0.0	0.0	0.3	0.3
Pb	0.88	0.01	0.0	0.0	0.0	0.0
Th	0.85	0.01	1668	474	1958	557
U	1.05	0.01	0.3	0.2	0.3	0.2

Figure 9. *Concentration ratios between wall rock, selvage, and vein.*

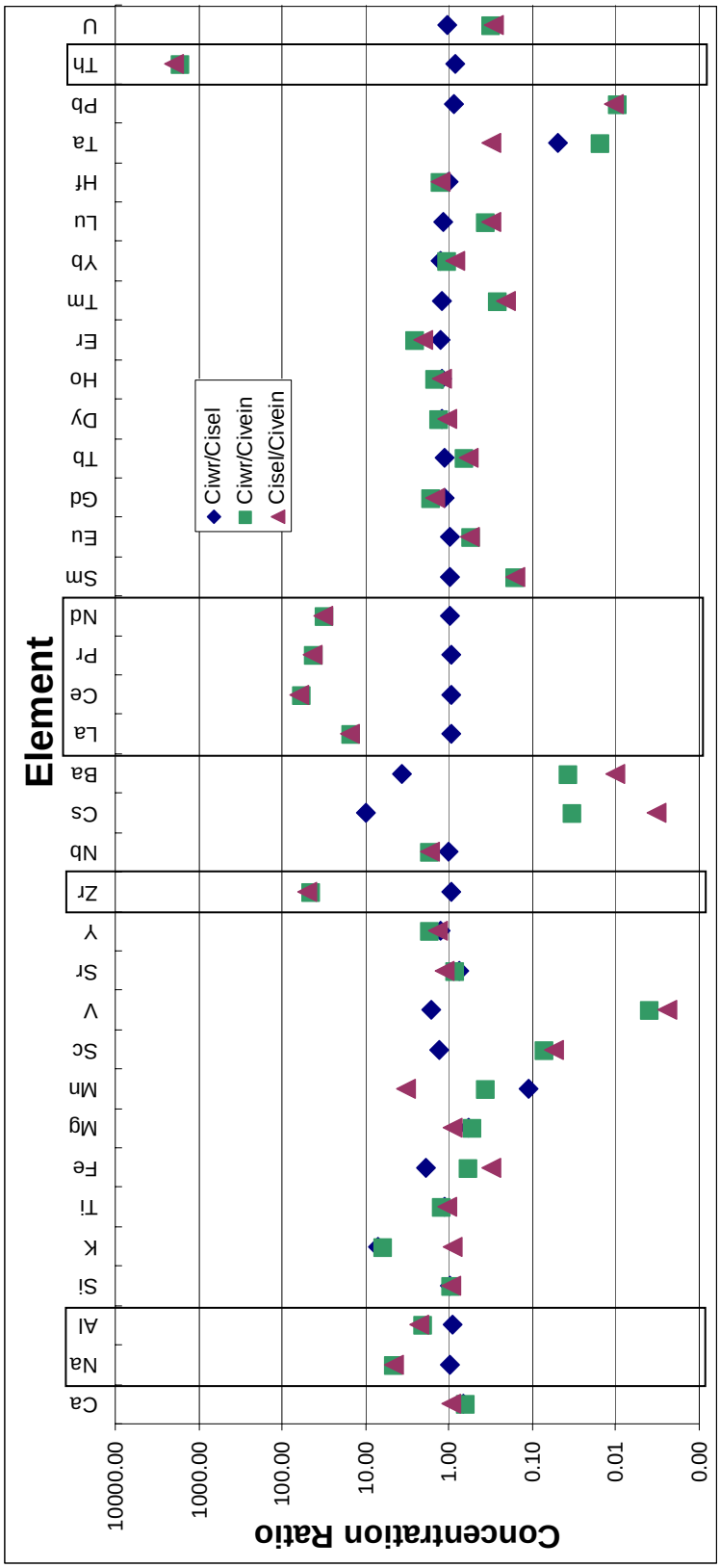

Figure 10. *Plotted concentration ratios.*

2008) and literature discussing solubility of these elements in metamorphic fluids of various compositions (Ague,2003).

The concentration ratios of the elements in this study were also considered to narrow the potential suite of IRFs. A chart of the concentration ratios for the elements considered in this study can be found in Figure 10. Similarities in the concentration ratios of the elements Na, Al, Th, Zr, La, Ce, Pr, and Nd suggest that they were mobilized similarly during vein fill and selvage alteration. These elements share a C_i^{wr}/C_i^{sel} that is below one, and very high C_i^{wr}/C_i^{vein} and C_i^{sel}/C_i^{vein} ratios. These ratios suggest that this suite of elements experienced little overall mobility, relatively small degrees of diffusion from the selvage to the vein, and either addition to the selvage by deposition from a metamorphic fluid or increased in composition in the selvage as a result of the loss of other material from the selvage.

Elements that best fit both of these considerations include Zr, Th, and the LREEs (La through Nd). In addition, the drastic decrease in Th and Ce concentrations (Th decreases ~200 fold and Ce decreases ~100 fold) within epidote in the vein relative to epidote in the selvage further suggest these elements did not diffuse into the vein nor did a metamorphic fluid deposit these elements in the vein/selvage assemblage. Other elements in this suite experience similarly drastic decreases in composition within epidote and other phases. This information can be found in Figures 7, 9, and 10.

A rough inverse correlation between C_i^{wr}/C_i^{vein} and C_i^{wr}/C_i^{sel} exists within this suite of elements. C_i^{sel}/C_i^{vein} can be used as a proxy for the diffusivity of an element under the supported assumption that these elements did not experience mobilization into or out of the system by a metamorphic fluid. Since we are relying on finding a perfectly immobile element to calculate the volume loss in the selvage, any mobility by diffusion will skew this calculation towards lower degrees of volume loss. Therefore, within this suite of elements, those with higher C_i^{sel}/C_i^{vein} values and lower C_i^{wr}/C_i^{sel} values are suggested to have experienced smaller degrees of diffused from the selvage to the vein and they should be preferentially considered for use as reference frames.

Thorium meets these criteria better than the other elements being considered; Ce is second, Zr is third, and the rest of the LREEs follow. A table of suggested volume losses based on the average concentrations of each potential immobile element can be found in Figure 11.

Wall rock heterogeneity can impart a large uncertainty to this volume loss calculation. This heterogeneity is included in the volume loss uncertainty reported in Figure 11. This heterogeneity was quantified by considering the C_i^{wr}/C_i^{sel} ratio of multiple wall rock and selvage bulk rock analyses. For each element considered for use in defining an immobile reference frame, this ratio strayed no more than ~5% above or below that element's average ratio. This heterogeneity is propagated into the two sigma uncertainty of each element in the mass balance equation.

	C_i^{WR}/C_i^{Sel}	2σ	ΔV	2σ
Th	0.85	0.042	15.0%	5%
Zr	0.92	0.043	8.0%	5%
La	0.95	0.043	5.1%	5%
Ce	0.93	0.043	6.5%	5%
Pr	0.95	0.043	4.7%	5%
Nd	0.97	0.044	3.0%	5%

Figure 11. *Potential IRF suite with C_i^{wr}/C_i^{sel} and suggested ΔV values.*

Volume Change in the Selvage

Decreased concentrations of sodium, potassium, and silicon and increased concentrations of aluminum, calcium, and titanium in the selvage relative to the wall rock are consistent with a selvage that has experienced loss of material mobilized in metamorphic environments. The former set of elements is documented to be mobile in metamorphic environments by previous studies while the latter set tends to act more refractory in these settings (Masters and Ague, 2005; Penniston-Dorland and Ferry, 2008). Additionally, the allanite component of epidote within the selvage increases with closer proximity the selvage/vein contact. The LREEs in allanite are considered very refractory in metamorphic environments (Ague, 2003; Penniston-Dorland and Ferry, 2008). This suggests that more material was mobilized closer to the contact. This observation is consistent with diffusion driven mobility across the selvage/vein contact into the vein.

An alternative interpretation would suggest that the selvage experienced an increase of volume by addition of aluminum, calcium, titanium, and the rare earth elements (REEs). This is unlikely considering the documented behavior of these elements in metamorphic environments (Ague, 1994; Masters and Ague 2005) and it requires material to travel up concentration and pressure gradients created by a proximal open fracture.

15% ± 5% volume loss in the selvage relative to the wall rock is used in this study. This corresponds to the average volume loss suggested by thorium and the maximum volume loss suggested by zirconium. These elements are preferentially considered based on how well they meet the criteria discussed in the 'Immobile Reference Frame Selection' section of this paper. Since some degree of thorium diffusion must have occurred (it is unrealistic to assume thorium is immune to diffusion) 15%± 5% is a minimum estimate of volume loss in the selvage.

Mass Balance Calculations

Selvage relative to Wall Rock (ΔC_i)

ΔC_i defines how much material was removed or added to the selvage relative to the wall rock corrected for volume change in the selvage. An element in excess in the selvage must have experienced deposition from a metamorphic fluid because diffusion would act to remove material from the selvage to the vein. An element depleted in the selvage could have experienced diffusion from the selvage into the vein and/or either mobilization and either removal by an infiltrating fluid or deposition from an infiltrating fluid. Figures 12 a and b contains a graphical representation of the ΔC_i values calculated in this study from bulk rock measurements.

Calcium, magnesium, manganese, strontium, and tantalum have positive ΔC_i values. These values are strong evidence that these elements have experienced deposition from a metamorphic fluid. The ΔC_i of Th is exactly zero. This is because the concentration ratio of thorium is being used to define the amount of volume change in the selvage relative to the wall rock. All other measured elements have negative ΔC_i values. These elements have been depleted from the selvage.

Mass Balance (C_i^{ext})

K, Zr, Ce, Pr, and Nd are depleted in the vein/selvage assemblage suggesting removal from the system during vein formation. Nb and La are indistinguishable from mass balance unity with error. V, Ba, Sc, Sr, Cs, Pb, Y, Sm, Gd, Tb, Dy, Ho, Er, Tm, Yb, Lu, Hf, Th, and U are in excess in the vein/selvage assemblage suggesting addition to the system during vein formation.

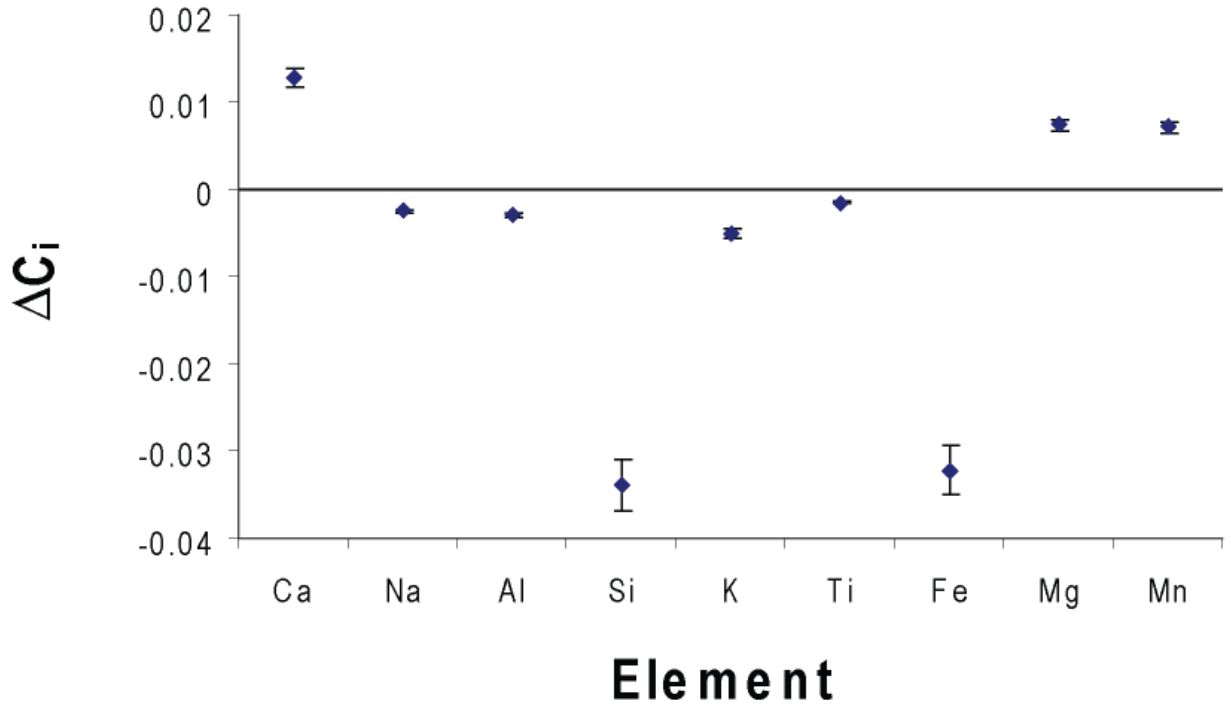

Figure 12a. *ΔC_i values for major elements considered in this study.*

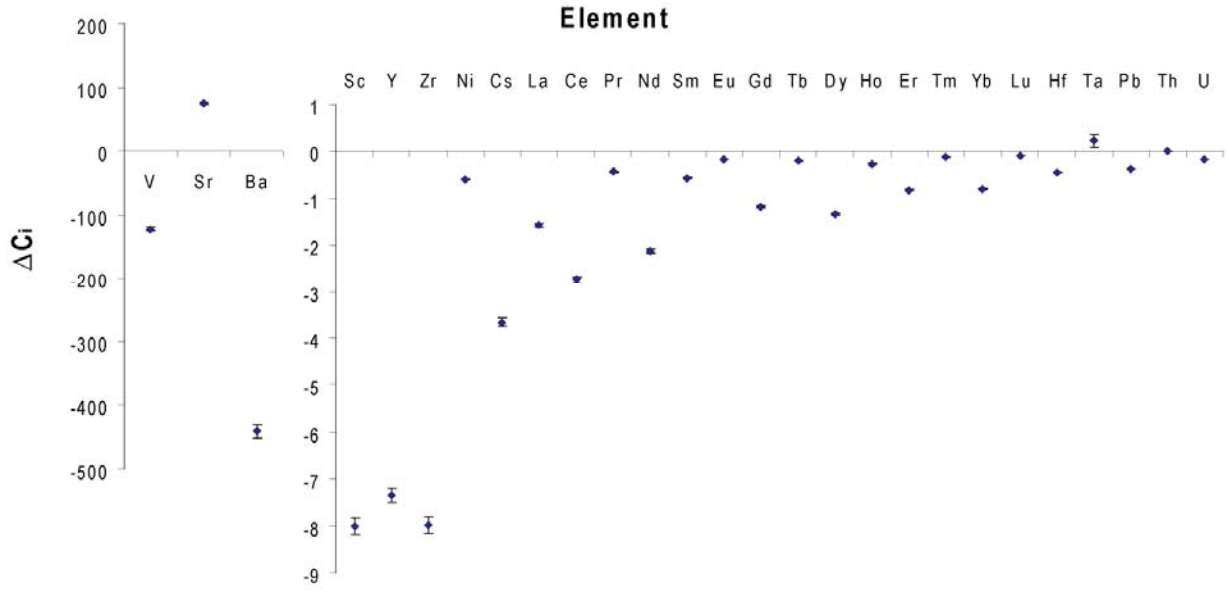

Figure 12b. *ΔC_i values for elements with trace compositions considered in this study.*

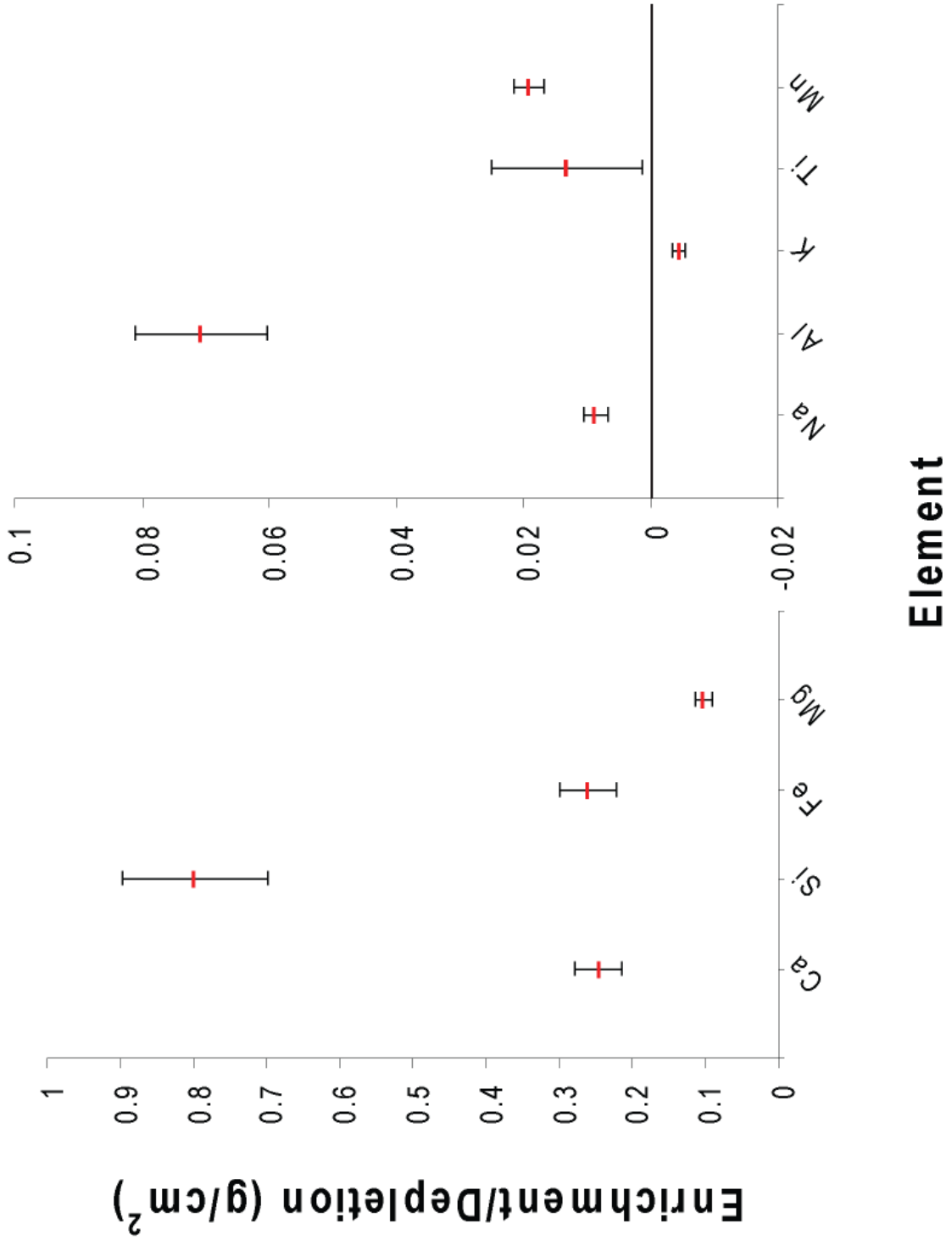

Figure 13a. *Results of the mass balance equation for rock forming elements considered in this study.*

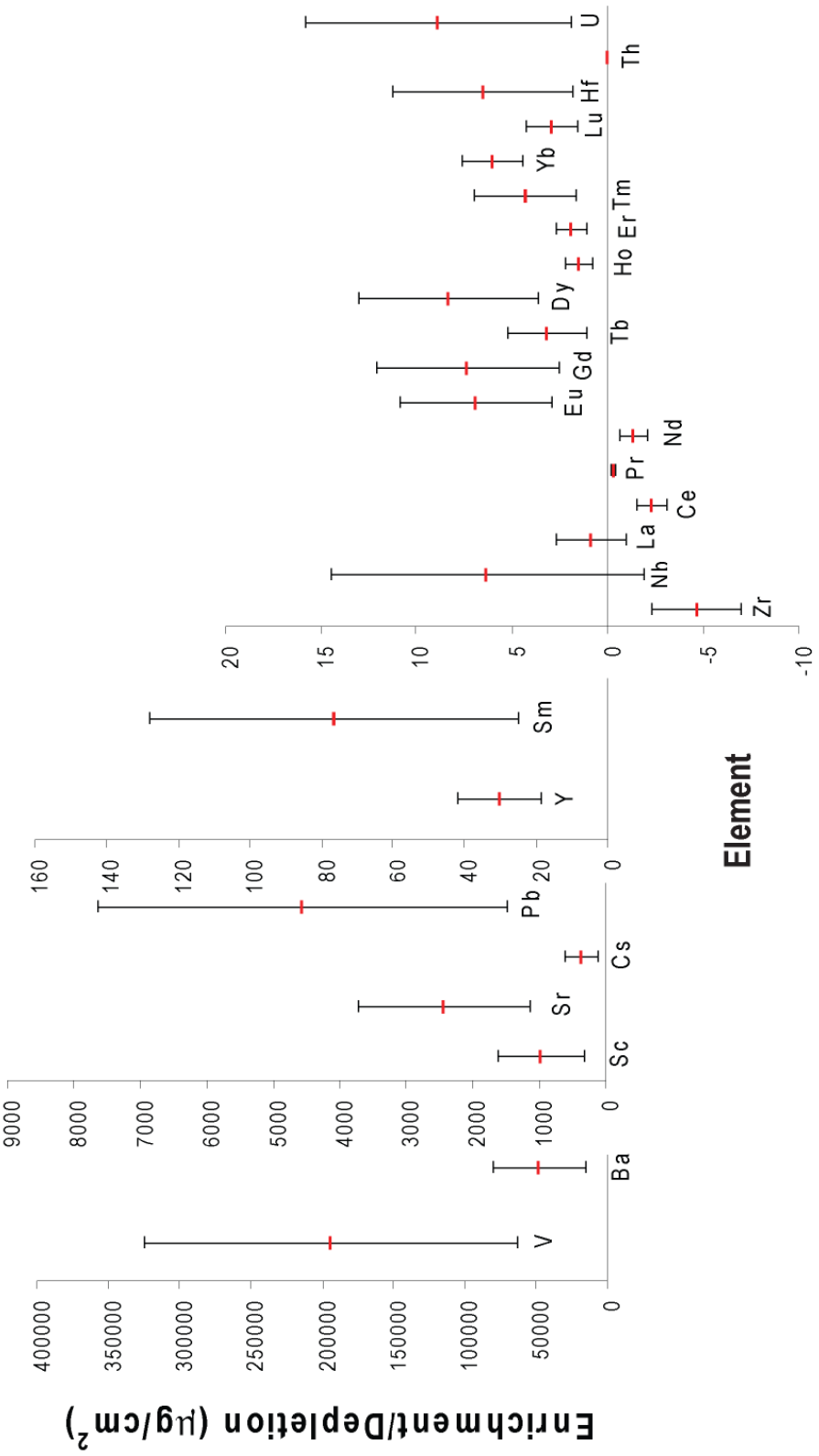

Figure 13b. *Results of the mass balance equation for trace element considered in this study.*

Presentation of these results can be found in Figures 13a and b.

Thorium plots with the elements with excess in the vein/selvage assemblage because thorium is used as the immobile reference frame in this study. The mass balance equation corrects volume change to this element. In doing so, any material in the vein is forced to be considered externally derived. It is much more likely that a large portion of this vein thorium represents diffusion from the selvage region. This assumption forces thorium into adherence of mass balance.

Elements found in excess in the vein/selvage assemblage likely experienced deposition via precipitation from metamorphic fluids traveling through the veins. Elements found to be depleted, experienced dissolution and removal by the metamorphic fluid during interaction with the surrounding wall rock. Elements found to adhere to mass balance are not suggested to have been effected by the metamorphic fluid by this study.

Conclusions

Rock forming elements (Ca, Na, Al, Si, K, Fe, Mg, Mn, and Ti) in these metavolcanic rocks from a contact metamorphic environment behave similarly in pelitic rocks in settings of regional metamorphism. Potassium depletion by metamorphic fluid infiltration is consistent with studies by Ague (1994) and Penniston-Dorland and Ferry (2008). Overall addition of silicon and calcium to the system corresponds with findings by Penniston-Dorland and Ferry (2008). These similarities suggest that rock-forming element behavior during fluid infiltration may not vary greatly between rock type and metamorphic settings. However these studies do not provide a basis for comparison across variations in temperature and pressure conditions.

Alkali metasomatism is commonly expressed as the exchange of sodium for potassium bearing phases or vice versa in a rock due to dissolution and removal of one and deposition of the other by an infiltrating metamorphic fluid (Ague, 2003). This can be indicative of the direction of flow of the metamorphic fluid (Ague, 2003). In these rocks, the elimination of biotite from the selvage, the removal of potassium from the vein/selvage assemblage, and the addition of sodium to the vein/selvage assemblage suggests that this phenomenon is occurring. Specifically, these observations support sodium metasomatism which is associated with up temperature gradient flow of chlorine bearing metamorphic fluid (Ague, 2003).

Elements plot on a spectrum on or between the end member cases: derived entirely from local processes and derived entirely from larger scale processes involving transportation with metamorphic fluids (see Appendix D). This measure can be plotted against C_i^{vein}/C_i^{wr}. This graph is provided in Figure 14 for rock forming elements in this study. This figure suggests a positive relationship between the abundance of an element in the vein and the percent of externally derived vein mass of that element.

A positive relationship between externally derived vein mass C_i^{vein}/C_i^{wr} suggests that larger degrees of mobility are increasingly dependent upon transport of mass into the vein via metamorphic fluids. This indicates that variation in diffusive potential among elements is smaller than variation in the potential for transport by metamorphic fluid among elements in this environment. Therefore, the mobility of an element in this vein fill situation is dominated by metamorphic fluid precipitation.

Future Work

Improvements to this study will be made by future work. Further attempts to locate biotite grains large enough to analyze

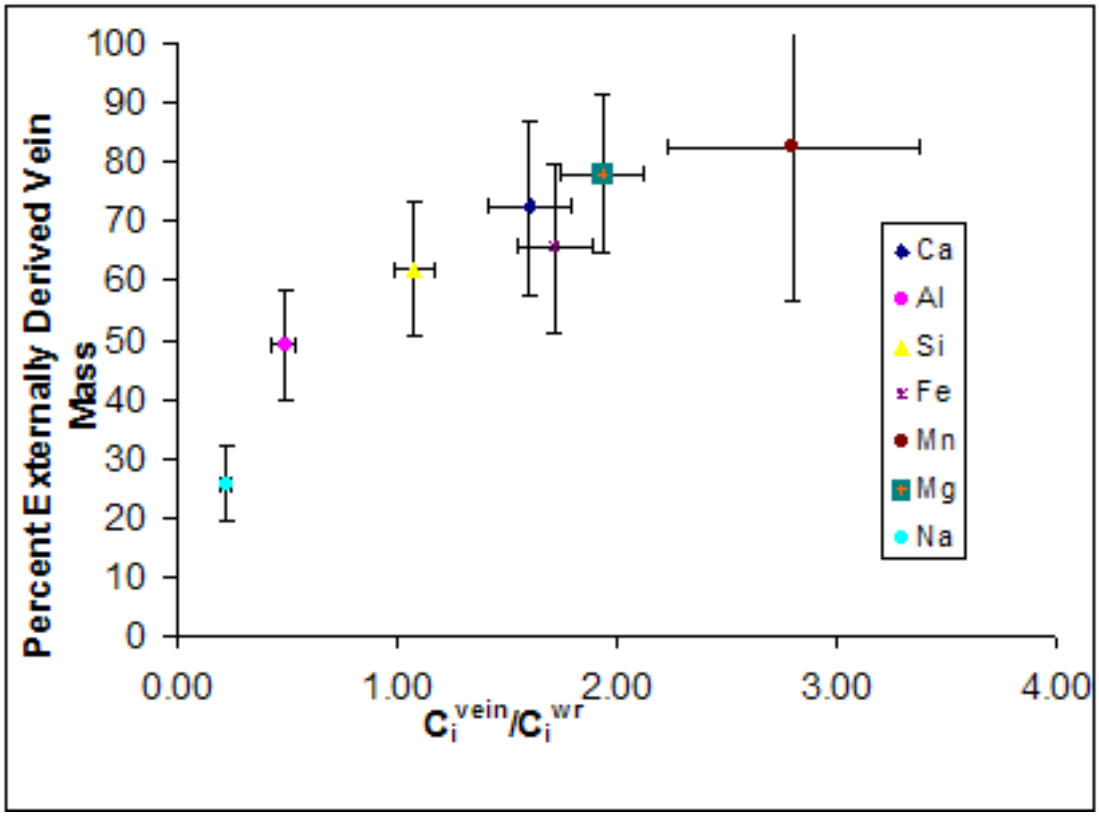

Figure 14. *Relationship between the percentage of externally derived mass in the selvage and vein and Civein/Ciwr as a proxy for overall mobility for elements experiencing enrichment in the vein/selvage assemblage.*

via LA-ICP-MS will be made. More vein point counting and phase analysis will better constrain vein bulk rock concentrations and decrease analytical uncertainties in the mass balance results. There is also potential for future work to expand on this study.

Measurements on additional veins from the same outcrop can be made to confirm the conclusions made by this study. Measurements on different types of veins from different localities within the same contact aureole can be made to better constrain the flow system as a whole.

Additionally, research to constrain the paleo-regional temperature gradients and timing of veining relative to intrusion. Studies may go about this by attempting to use titanite found the vein to calculate U-Pb age of vein fill.

A detailed look at the potassium and sodium mobility and fluid inclusion analysis to constrain the chlorine content of infiltrating metamorphic fluid may yield information about the direction of flow relative to the temperature gradients associated with the intrusion. If sodium metasomatism is occurring then metamorphic fluid is suggested to be traveling up thermal gradient (Ague, 2003).

Eventually, continued effort could lead to constraints on regional time integrated fluid fluxes through various sets of veins in the region. An integrated understanding of the history of veining and the structural development of the Ritter Range Roof Pendant could yield a deep understanding of fluid flow in metamorphic and meteoric origins.

Acknowledgements

This study would not have been possible without the constant support of Dr. Penniston-Dorland or the guidance, advice, and instruction of Dr. Ash, Dr. McDonough and Dr. Piccoli. Additionally, funding and advice for field localities were provided by Dr. Sorensen of the Smithsonian Institute.

Supplementary Material

Electron Probe Micro Analysis (EPMA)

EPMA utilizes an electron beam to quantitatively analysis the chemistry of solid samples. The beam is generally generated by a tungsten filament cathode and focused towards the sample by a positively charged anode and a series of magnets and apertures. The resultant beam is general between one and three microns in diameter. Interaction with the sample causes heat, visible light fluorescence, x-ray emission, secondary electron emission, backscatter electron emission, and Auger electron emission.

Measurement of backscatter electron production can be used to generate raster images useful for recognizing phases and textures in the sample. X-ray emission is analyzed by either wavelength dispersive or energy dispersive methods to provide quantitative chemical composition measurements. These measurements can be made as at as low as the one hundred parts per million (ppm) level. More commonly these measurements are made at an accuracy of around ten thousand ppm.

Quantitative chemical composition analysis requires the use of standard materials of known compositions to be used as references. Ideally these references have similar crystal structure and composition as the unknown. In this study, this requirement was met by using either standards of the same mineral type as those measured.

Laser Ablation Inductively Coupled Plasma Mass Spectrometry (LA-ICP-MS)

ICP-MS utilizes argon gas plasma to generate ions from an introduced sample. The sample is then moved into a mass spectrometer which focuses and accelerates the ionized sample via a series of positively charged anodes, magnets and apertures. The sample is then differentiated by charge and mass by an electromagnet. Ions are then further collimated and focused into a detector. Measurements can be made as low as the part per trillion level for some elements.

Laser Ablation is a method of solid sample introduction into an ICP-MS. This method utilizes a high laser flux to cause material excavation of a sample with limited heating of the sample. Excavated material is swept via pump into the plasma sector of an ICP-MS. Laser ablation allows for very specific regions (as small as a three micron diameter spot) of a sample to be measured. This is useful with geologic samples which often deal with small grains of material.

Quantitative composition analysis for LA-ICP-MS requires the use of a standard material in which all elements of interest are present and preferably have concentrations in the comparable to those in the sample. The concentration of an element in the sample must be known. NIST610 was used for all phases, BCR2 was used as an unknown standard for silicate phases to check the measurements. Calcium was used as the known element for all phases but ilmenite. Manganese was used as the known element for ilmenite. The concentration of these elements in measured phases was obtained through WDS-EPMA.

Appendix A

Field Measurements

	Thickness (cm)	Volume %
Quartz Veins	18.4	1.1
Amphibole Veins	10.2	0.6
Amph/Qrtz Veins	23.2	1.3
Vein Selvage	36.8	2.1
Epidote Pod	28.6	1.7
Epidote Pod Margin	3.5	0.2
Wall Rock	1600.8	93.0
Total Vein	51.8	3.0
Vein Selvage	36.8	2.1
Total Thickness	1721.5	100

	Average Length (cm)
Quartz Veins	34
Amph/Qrtz Veins	178
Amphibole Veins	37

Average Length of Selvaged Veins
264 cm
Average Thickness of Selvaged Veins
0.7 cm
Average Vein/Selvage Thickness Ratio
0.9 cm

***Uncertainties not reported.

Appendix B

Plagioclase Ternary Diagram

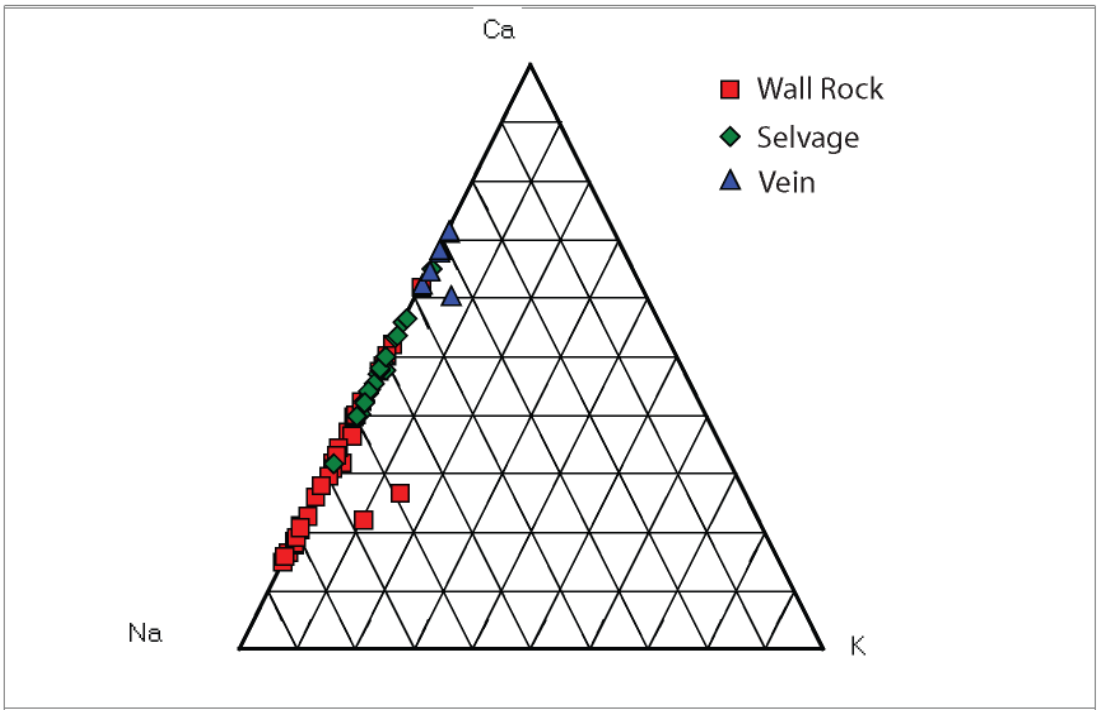

Appendix C

Oxide Weight Percent for Selvage and Wall Rock Material

	Selvage		Wall Rock	
	Wght%	Variability	Wght%	Variability
SiO_2	56	2	55	2
Al_2O_3	20.9	0.7	18.9	0.7
Fe_2O_3	4.5	0.5	8	1
MgO	1.2	0.2	2.6	0.5
CaO	10	1	6.5	0.7
Na_2O	5.0	0.2	4.9	0.2
K_2O	0.20	0.09	1.4	0.6
TiO_2	0.90	0.03	1.02	0.03
P_2O_5	0.2	0.0	0.26	0.00
MnO	0.120	0.006	0.137	0.007
Cr_2O_3	0.04	0.02	0.04	0.02
LOI	1.1	0.1	0.8	0.1

Appendix D

Percent Excess Material in Vein/Selvage Assemblage by Element

	% Excess	2σ error		% Excess	2σ error
CaO	75	14	Ce	-5	3
Na_2O	22	6	Pr	-5	3
Al_2O_3	46	9	Nd	-5	3
SiO_2	65	11	Sm	92	87
K_2O	-113	29	Eu	77	61
TiO_2	57	67	Gd	48	40
FeO	74	15	Tb	72	63
MgO	78	13	Dy	54	39
MnO	84	21	Ho	51	30
Sc	96	90	Er	31	15
V	100	95	Tm	88	75
Sr	69	53	Yb	60	20
Y	45	21	Lu	83	54
Zr	-3	3	Hf	57	55
Nb	49	85	Ta	98	102
Cs	99	94	Pb	100	95
Ba	98	94	Th	0	5
La	3	7	U	86	93

*negative values indicate a net loss of material. Values are given as the percent of lost material relative to total initial material.

BIBLIOGRAPHY

Ague, J (1994).Mass transfer during barrovian metamorphism of pelites, south-central conneticut. 1: evidence for changes in composition and volume. *American Journal of Science*. 294, 989-1057.

Ague, J (2003).Fluid Flow in the Deep Crust. *Treatise on Geochemistry*. 3, 195-228.

Baumgartner, L and Olsen, S (1995). A least-squares approach to mass transport calculations using the isocon method. *Economic Geology*. 90, 1261-1270.

Grant, J (1986).The isocon Diagram – a simple solution to Gresens' Equation for Metasomatic Alteration. *Economic Geology*. 81, 477-1976-1982.

Gresens, R (1966).Composition-Volume relationships of metasomatism. *Chemical Geology*. 2, 47-65.

Hanson, B (1993).Long term evolution of fluid-rock interactions in magmatic arcs;evidence from the Ritter Range pendant, Sierra Nevada, California and numerical modeling. *Journal of Petrology*. 34, 23-62.

Holland, T and Powell, R (1998).An internally consistant thermodynamic data set for phases of petrological interest. *Journal of Metamorphic Geology*. 16, 309-343.

Masters, R and Ague J (2005).Regional-scale fluid flow and element mobility in Barrow's Metamorphic zones, Stonehaven, Scotland. *Contributions to Mineral and Petrology*. *150*, 1-18.

Oliver, N and Bons, P (2001).Mechanisms of fluid flow and fluid-rock interaction in fossil metamorphic hydrothermal systems inferred from vein-wallrock patterns, geometry and microstructure. *Geofluids*. *1*, 137-162.

Oliver, N (1996).Review and classification of structural controls on fluid flow during regional metamorphism. *Journal of Metamorphic Geology*. 14, 477-492.

Penniston-Dorland, S and Ferry, J (2008).Element mobility and scale of mass transport in the formation of quartz veins during regional metamorphism of the Waits River Formation, east-central Vermont. *American Mineralogist*. 93, 7-21.

Pyle, J., Spear, F., Rudnik, R., McDunough, W.. (2001). Monazite-xenotime-garnet equilibrium in metapelites and a new monazite-garnet thermometer. *Journal of Petrology*. 42, 11, 2083-2107.

Sorensen, S Dunne, G, Hanson, RB, Barton, M, Becker, J, Tobisch, O, Fiske, R (1998). From Jurassic shores to Cretaceous plutons: geochemical evidence for paleoalteration environments of metavolcanic rocks, eastern California. *GSA Bulletin*. 110, 326-343.

Van Der Plas and Tobi (1965).A chart for judging the reliability of point counting results. *American Journal of Science*. 263, 87-89.